Excitonic recombination and absorption in $In_xGa_{1-x}As$/GaAs heterostructure nanowires

Marta De Luca,[1] Giovanna Lavenuta,[1] Antonio Polimeni,[1] Silvia Rubini,[2] Vincenzo Grillo,[3] Francesco Mura,[4] Antonio Miriametro,[1] Mario Capizzi,[1] and Faustino Martelli[5,*]

[1]*Dipartimento di Fisica, Sapienza Università di Roma, piazzale A. Moro 2, 00185 Roma, Italy*
[2]*TASC-IOM-CNR, Area Science Park, S.S. 14, Km. 163.5, 34149 Trieste, Italy*
[3]*Istituto Nanoscienze-S3 CNR, via Campi 213/A, 41125 Modena, Italy and IMEM CNR, I-43100 Parma, Italy*
[4]*Dipartimento di Scienze di Base e Applicate per l'Ingegneria, Sapienza Università di Roma, via Scarpa 16, Roma, Italy*
[5]*IMM-CNR, via del Fosso del Cavaliere 100, 00133 Roma, Italy*

(Received 13 February 2013; published 10 June 2013)

Photoluminescence (PL), micro-PL, and PL excitation (PLE) spectroscopy for different light polarizations have been used to investigate the electronic properties of GaAs characterized by a dominant wurtzite (WZ) phase that forms in bare GaAs and in InGaAs/GaAs heterostructure (HS) nanowires (NWs). In both cases, the GaAs luminescence exhibits very narrow emission lines, which persist up to room temperature. At 10 K, the energy of the exciton ground state recombination of GaAs NWs is equal to 1.522–1.524 eV. In HS NWs, micro-PL combined with transmission electron microscopy pinpoints the tip of the GaAs section, with a dominant WZ phase, as the origin of that emission. In PLE, two very narrow excitonic absorptions at 1.523 and 1.631 eV involve different critical points of the WZ valence band (Γ_{9v} and Γ_{7vu}). The low-energy peak shows a negligible Stokes shift with respect to PL. At 10 K, a further weak and broad PLE signal is found at 1.59 eV. The possible attribution of these lines within the present knowledge of the WZ band structure is critically discussed.

DOI: 10.1103/PhysRevB.87.235304 PACS number(s): 78.67.Uh, 78.55.Cr, 78.66.Fd, 61.46.Km

I. INTRODUCTION

Despite the research on GaAs nanowires (NWs) which has been ongoing for more than a decade, the optical properties of these promising nanostructures are far from being well known. The large surface-to-volume ratio with the ensuing oxidation issues, the difficulty of having NWs with a high-quality lattice structure, and possible contamination from the metals used to seed the growth are among the reasons for the poor knowledge of the optical properties of GaAs NWs. In particular, the relatively low crystal quality of GaAs NWs arises from the coexistence of wurtzite (WZ) and zinc-blende (ZB) phases in the lattice structure of individual NWs.[1] This occurrence has been observed in other III-(As,P) NWs, too, and is a surprising observation in these technologically relevant nanostructures. The WZ lattice structure, indeed, can be hardly found in bulk III-(As,P) semiconductors, and its existence is a topic of fundamental interest in materials science. Optical measurements from pure WZ GaAs NWs need to be reported, although stacking-fault-free WZ GaAs NWs with a very thin diameter have been obtained.[2] The variety of WZ-ZB lattice mixtures obtained in different laboratories is the main reason for the different results reported in the literature, in particular, for the energy spread in the NW band-gap energy. On the other hand, the coexistence of WZ and ZB phases in the same NW gives the possibility to fabricate fascinating WZ/ZB heterostructures aligned along the wire axis.[3] Despite these interesting motivations, several electronic properties of these NWs are still not well assessed. Probably the most complete picture has been obtained by optical measurements in InP, where the band-gap energy of the WZ phase has been determined to be 70 meV greater than that of the ZB phase,[4–6] in good agreement with theoretical predictions.[4]

As mentioned, optical measurements in GaAs NWs have given quite different results. Photoluminescence (PL) measurements in WZ-containing GaAs NWs show that the highest emission energies fall in two distinct energy ranges: from 1.510 to 1.525 eV, namely, slightly below or 10 meV above the ZB phase,[7–13] or from 1.545 eV to less than 1.590 eV.[14–16] Cathodoluminescence[15] and resonant Raman scattering[17] (RRS) suggest a WZ band gap in this last energy range. However, other RRS measurements suggest a band gap at 1.516 eV,[18] or find only a resonance 100 meV above that belonging to the ZB phase.[19] Very recently, WZ GaAs epitaxially grown on ZB GaAs (100) was accidentally obtained,[20] but the sample could not be reproduced. Room temperature surface photovoltage (PV) measurements on that sample indicate band-gap-related features at 1.44 eV for the WZ phase and 1.37 eV for the ZB phase.[20]

For all theoretical investigations, the lowered crystal symmetry of WZ GaAs with respect to the ZB phase leads to a Γ_{9v}, Γ_{7vu}, and Γ_{7vl} ladder in the valence band (VB), in order of increasing *hole* energy. As for the conduction band (CB), the increase in the lattice constant along one of the [111] axes, namely, the WZ $\hat{c}$ axis, results in a folding of one L_{6c} conduction band minimum of the ZB phase onto an additional Γ_{8c} minimum in the WZ phase, which gives rise to a different pseudodirect transition. Although the relative energy ordering of Γ_{8c} and Γ_{7c} is debated, in the most accepted view the fundamental band gap results from a Γ_{9v}-Γ_{7c} transition allowed only for light polarized perpendicular to the $\hat{c}$ axis.[21,22] Different developments of first principles *ab initio* pseudopotential methods within the local density approximation and calculations in the GW approximation[23–28] estimate values of the energy gap for the WZ phase of GaAs (and of its energy difference with respect to the ZB phase, $\Delta E_{\text{WZ-ZB}}$) that range from 0.47 eV ($\Delta E_{\text{WZ-ZB}} = 0.03$ eV)[23] to 1.861 eV ($\Delta E_{\text{WZ-ZB}} = 0.087$ eV).[27] These values depend on the theoretical or experimental value of the c/a ratio used (c and a being the lattice constant parallel and perpendicular to the WZ $\hat{c}$ axis, respectively), an issue presently a matter in theoretical and experimental studies. Furthermore, an extended-basis *spds** first-neighbor tight-binding model estimates an optical band-gap energy equal to 1.533 eV ($\Delta E_{\text{WZ-ZB}} = 0.014$ eV).[29] Finally, it has been reported also that the presence of both WZ and ZB phases in the same wire may lead to a type-II band alignment of WZ and ZB phases with an ensuing recombination among electrons confined in the ZB sections of the NW and holes in the WZ sections.[26,30]

In this paper, we present PL, micro-PL (μ-PL), and PL excitation (PLE) measurements in GaAs NWs grown by molecular beam epitaxy (MBE) on GaAs substrates and characterized by scanning and transmission electron microscopy. In all samples, an intense and extremely narrow PL peak has been observed in the 1.522–1.524 eV energy range. μ-PL measurements show that this peak originates from the NW tips, where the GaAs WZ phase is dominant except for a limited number of stacking faults. At 10 K, PLE spectra display two distinct, strong, and narrow excitonic peaks with average energies 1.523 and 1.631 eV, which persist up to room temperature, and a further, much weaker, and broader band at about 1.59 eV. All these measurements, together with polarization-resolved measurements of the emitted light for different geometries of laser excitation and luminescence collection, would point toward an attribution of the two stronger emissions to well defined transitions involving the Γ_{9v} and Γ_{7vu} VB states of WZ GaAs. Our results are framed within the existing experimental and theoretical results and possible attributions of the observed transitions are critically discussed.

II. EXPERIMENTAL DETAILS

Samples investigated here are Au-induced bare GaAs NWs and $In_xGa_{1\text{-}x}As$/GaAs heterostructure (HS) NWs grown by MBE at 580 and 500 °C, respectively. The HS NWs were grown as described in Ref. 30: After InGaAs, GaAs is grown that forms both a shell around the InGaAs section and an axial GaAs section on top of the InGaAs. These HS NWs allowed us to get an enhanced InGaAs emission and improve the optical quality of the GaAs section forming at the NW tip,[31] as shown in the following. Several samples with In concentrations ranging from $x = 0.03$ to 0.30, as obtained by the known compositional dependence of the band-gap energy in bulk unstrained InGaAs,[32] were grown on GaAs(111) substrates. Self-induced ZB NWs grown on GaAs(100) substrates were also studied for comparison purposes. The samples were morphologically and structurally characterized by scanning electron microscopy (SEM) and transmission electron microscopy (TEM). PL was excited by a frequency-doubled Nd:YVO_4 laser, which also served for pumping a tunable Ti:sapphire laser used for PLE measurements. The luminescence was spectrally analyzed by a double 0.75 m monochromator and detected by either a N-cooled Si CCD, or an InGaAs linear array, a Ge photodiode, or a GaAs photomultiplier for single photon counting. Laser wavelength and power, measured by a Michelson interferometer and a calibrated Si photodiode, respectively, were acquired automatically during PLE measurements, together with the luminescence signal. PL and PLE measurements were performed from 10 K to room temperature by using a closed-cycle cryostat, with the laser spot size (roughly 200 μm in diameter) exciting about 5×10^5 NWs. Different excitation and detection geometries were exploited in order to address polarization-related selection rules, as specified in due course. All measurements were made insensitive to the polarization response of the optical setup by using both a linear polarizer and a liquid crystal variable retarder. Micro-PL (μ-PL) was performed using a $50\times$ microscope objective with a 0.55 numerical aperture (with a resulting spot size equal to about 1 μm). For these measurements the nanowires were transferred mechanically on a Si substrate in order to acquire μ-PL maps of isolated, single NWs held at $T = 5$ K and moved by a computer-driven piezoelectric translation stage.

III. RESULTS

Figure 1 displays the 10 K PL spectra, recorded in a backscattering geometry (namely, laser beam and luminescence detection are both parallel to the wire axis

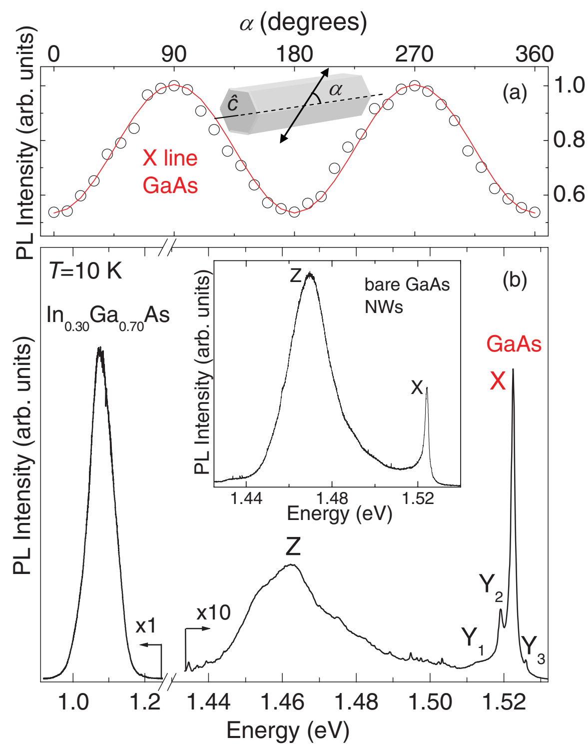

FIG. 1. (Color online) (a) PL spectrum of a heterostructure $In_xGa_{1\text{-}x}As$/GaAs NW ($x = 0.30$) sample. Notice the axis break and change of scale on the abscissa axis. The measurement was recorded in a backscattering geometry (laser beam and luminescence detection are both parallel to the wire axis but with opposite directions). The band at 1.08 eV is due to electron-hole recombination in the $In_{0.30}Ga_{0.70}As$ section. X indicates a free-exciton recombination in GaAs. Weak lines Y_1, Y_2, and Y_3 saturate with respect to the X line for increasing laser power density and/or lattice temperature. 10 K PL of a bare GaAs NW sample is shown in the inset. In all samples, band Z decreases in intensity with respect to band X with increasing excitation power and/or lattice temperature. (b) Dependence of the PL intensity of line X on the angle α between the wire $\hat{c}$ axis and the axis of a linear polarizer (see the inset). The red solid line is a fit of light intensity to $I = a + b\sin^2(\alpha)$. PL, collected perpendicularly to the $\hat{c}$ axis, is polarized prevalently perpendicularly to the wire $\hat{c}$ axis, as expected for wurtzite GaAs.

but with opposite directions) of two representative samples investigated here. These samples are structurally characterized by a predominant WZ phase, as determined by TEM images to be displayed in the following. Figure 1(a) shows the PL of $In_xGa_{1-x}As/GaAs$ ($x = 0.30$) HS NWs grown on a GaAs(111) substrate. Several emission bands characterize this PL spectrum. The intense and broad band, peaked at 1.075 eV, is attributed to electron-hole recombination in $In_xGa_{1-x}As$ on the grounds of the dependence of its peak energy on In concentration. The broad and structured band Z, peaked at 1.462 eV with a shoulder at ∼1.454 eV, saturates with laser power and quenches for $T > 60$ K. In previous works, recombination bands at similar energies have been attributed either to an ensemble of unresolved type-II transitions[33] or to defect-related transitions involving C atoms.[15] The X emission—whose peak energy changes by ∼2 meV from sample to sample—is very narrow [full width at half maximum (FWHM) equal to 0.8 meV in the best cases, as in Fig. 4(a)] and persists up to room temperature (RT): This emission is attributed to a free-exciton (FE) recombination in WZ GaAs. Finally, the Y_n lines ($n = 1,2,3$)—located at 1.513 eV, as more evident in other spectra, 1.519 and 1.526 eV—vanish as soon as the lattice temperature exceeds 30 K. The 1.526 eV line has been observed only in limited regions of the sample and could not be reproduced over time. The other two lines fall in an energy range where a number of similar narrow lines, attributed to excitons bound to stacking faults, have been already reported.[15]

The inset shows the PL spectrum of a bare GaAs NWs grown on GaAs(111). Only two emission bands characterize this spectrum. The strong, low-energy Z band, peaked at 1.469 eV, behaves as the band observed at 1.462 eV in the HS NW sample: Its intensity decreases relative to that of the higher-energy X band with increasing temperature and/or excitation power. The high-energy narrow X band (FWHM = 2.0 meV and peaked at 1.524 eV) persists as narrow and intense up to room temperature, despite the absence of a shell: It is attributed, therefore, to free-exciton recombination in WZ GaAs. Notice that this band, which is broader but still well defined, is observed also in HS NWs grown on Si substrates.

A comment on the optical quality of the material is now in order. The FWHM of the X band is quite narrower and the ratio between its intensity and that of the impurity-related band at about 1.46 eV in HS $In_xGa_{1-x}As$ NWs is quite higher than in bare GaAs NWs. These features indicate that the optical quality of GaAs is much better in HS NWs than in bare GaAs NWs, most likely because a buffer action of the $In_xGa_{1-x}As$ section leads to a lower incorporation of impurities in GaAs.

The attribution of the X band to a recombination involving WZ GaAs (in particular, the WZ valence band) is confirmed by the data shown in Fig. 1(b), where the dependence of the X-band intensity on the angle α between the symmetry axis $\hat{c}$ of the NWs and the axis of a linear polarizer is shown by circles. These measurements were performed with the laser beam parallel to the $\hat{c}$ axis (namely, perpendicular to the substrate plane), while the luminescence was collected from the sample edge, that is, from the NW side (see the inset). This configuration enables to select emitted light polarized either parallel or orthogonal to $\hat{c}$. The light intensity data are fit well by $I = a + b\sin^2(\alpha)$ (red solid line), with a maximum of the PL intensity when the polarizer axis is perpendicular to the NW axis ($\alpha = 90°$). This polarization is characteristic of an emission from WZ NWs, while it is opposite[5,34] to that of the emission from ZB NWs. In addition, the intensity of the Z and Y_2 recombinations follows the same angular dependence of the X band, thus indicating that all these emissions involve WZ-related electronic levels.

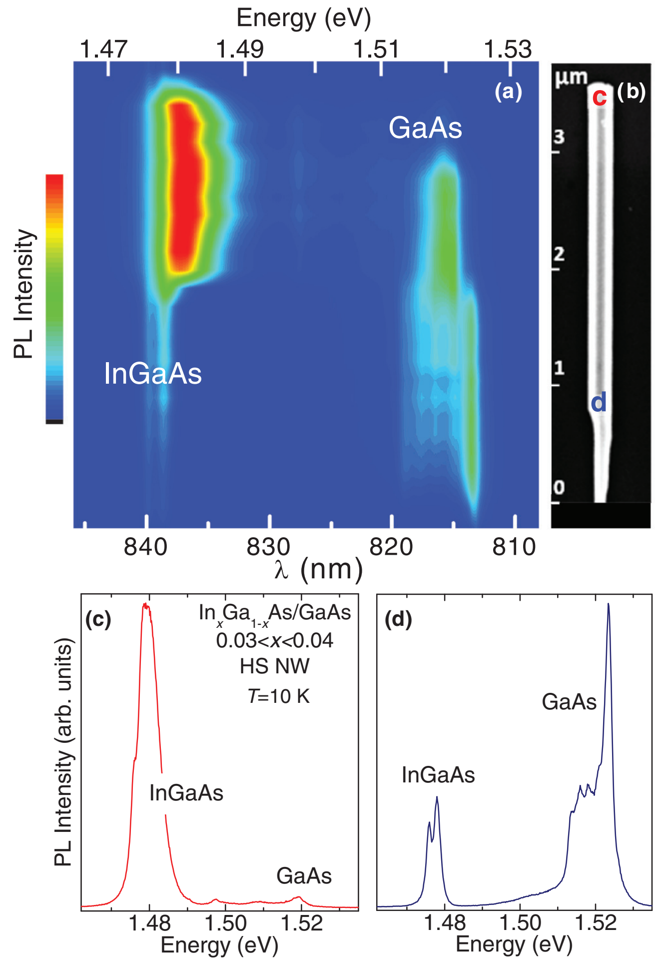

FIG. 2. (Color online) (a) Low-temperature ($T = 10$ K) μ-PL map of the emission intensity of an $In_xGa_{1-x}As$ ($0.03 < x < 0.04$) heterostructure NW, ∼3.5 μm long. The measurement was recorded in a backscattering geometry (the laser beam was orthogonal to the substrate and the luminescence was collected along the same direction of the laser). The abscissa scale indicates the energy of the PL emission, whose intensity is given in a false color scale shown on the left. The ordinate scale refers to the position of the laser spot on the NW, whose corresponding SEM image is shown in (b). (c) μ-PL spectrum recorded on point (c) indicated in (b). (d) μ-PL spectrum recorded on point (d) indicated in (b).

In order to address the spatial origin of the narrow X peak, we performed μ-PL on single NWs mechanically transferred on a Si substrate, with the laser beam orthogonal to the substrate and the luminescence collected along the same direction of the laser. In Fig. 2(a), the PL intensity emitted from different regions of an $In_xGa_{1-x}As/GaAs$ ($0.03 < x < 0.04$) HS NW, ∼3.5 μm long, is shown in a false color map. A corresponding SEM image of the investigated NW is shown in Fig. 2(b).

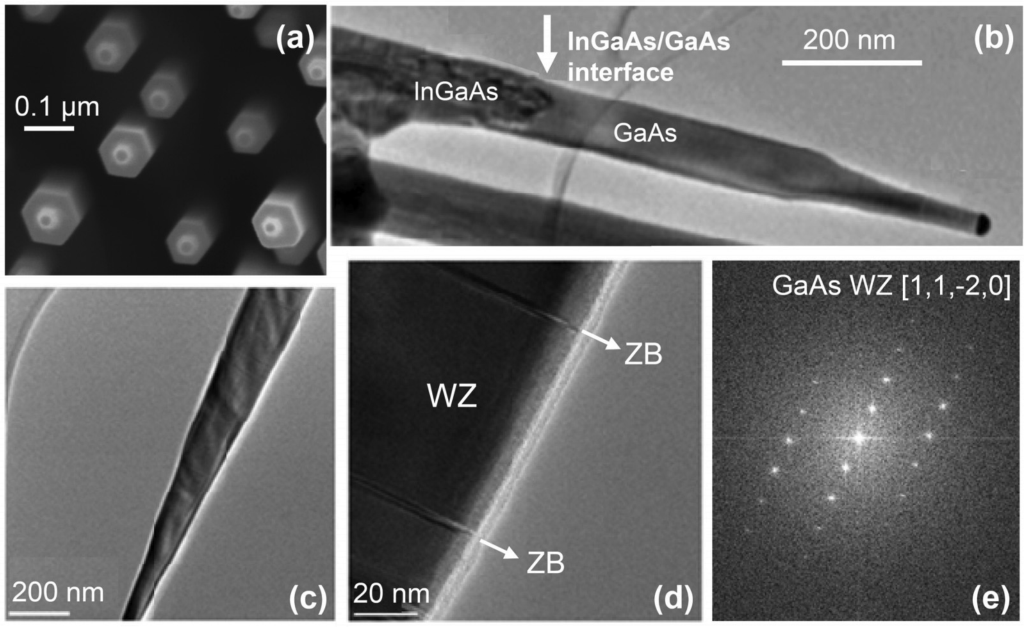

FIG. 3. (a) SEM image showing a top view of the hexagonal structure of a few $In_xGa_{1-x}As$/GaAs heterostructure ($x = 0.30$) NWs. (b)–(d) TEM images at increasing magnification of an $In_xGa_{1-x}As$/GaAs HS ($x = 0.30$) NW. In (b), the arrow indicates the end of the InGaAs section. (c) and (d) show a nearly defect-free region close to the wire tip characterized by WZ GaAs with occasional ZB insertions. (e) shows the diffractogram taken in the tapered part of the wire which exhibits a hexagonal symmetry.

Near the NW base, light is emitted in the energy range of both the $In_xGa_{1-x}As$ section (∼1.48 eV) and the GaAs section (∼1.52 eV) [see the PL spectrum shown in Fig. 2(c)]. The latter emission is probably due to type-II and/or defect-related transitions.[15] On moving toward the NW tip, the InGaAs emission—at lower energy—decreases in intensity while the GaAs emission—at higher energy—gains in intensity, as displayed in Fig. 2(d). Most importantly, the PL GaAs emission is peaked at higher energy and narrows on going from the base to the tip of the NW, and is finally equal to 1.524 eV (FWHM $\leqslant$ 2 meV) at the extreme tip of this NW. This abrupt energy variation takes place at about 1.8 μm from the wire base and is related to a change in the crystal phase of GaAs, consistent with TEM measurements (see the following).

Figure 3 shows SEM and TEM images of a typical $In_{0.30}Ga_{0.70}As$/GaAs HS NW (that is, the same sample whose PL and PLE spectra are shown in Figs. 1 and 4, respectively). Figure 3(a) displays a top-view SEM image of a few NWs having a hexagonal structure expected for growth on (111) substrates. TEM images of a single NW for an increasing magnification of the same sample section are shown, instead, in Figs. 3(b)–3(d). In the core-shell region, the NW structure is mainly hexagonal, occasionally with a large number of defects that make the identification of the phase less univocal. On the contrary, the NW tip is *nearly defect free* and is characterized by extended WZ GaAs regions intercalated by occasional and tiny ZB GaAs inserts, as shown in Figs. 3(c) and 3(d) and supported by the diffractogram in the tapered part of the NW shown in Fig. 3(e). A similar structure has been previously found in $In_{1-x}Ga_xAs$/GaAs NW samples similar to those investigated here.[31,35]

These TEM images and μ-PL measurements indicate a large contribution to the PL spectra of Fig. 1 from carrier recombination in the tip, a pencil-like part of the NW—namely, in regions with dominant WZ GaAs with small inserts of ZB GaAs. This strong signal from NW tips observed in macro-PL in a backscattering configuration with the exciting laser beam parallel to the NW axis is due mainly to a laser light absorption that takes place mostly close to the NW tip because of multiple reflections by individual wire surfaces.[36,37] In turn, this explains why no ZB GaAs emission is observed in macro-PL from the substrate. This is consistent with the black surface of these samples. On the contrary, excitation and the observation of states related to the whole NW can be attained in the μ-PL configuration, where the NW is lying horizontally and can be excited alongside and its luminescence detected without being absorbed by other surrounding nanowires.

In order to ascertain the intrinsic nature of the observed emissions, PLE measurements have been performed. These measurements mimic absorption and are thus related to the material density of states. Typical PL (black dashed line) and PLE (blue solid line) spectra recorded in a backscattering geometry (same as described for Fig. 1) at 10 K in a HS $In_{0.30}Ga_{0.70}As$/GaAs sample are shown in Fig. 4(a). The detection energy is set at the Y_2 line (1.519 eV). The PLE spectrum exhibits two sharp peaks, at 1.522 eV (A) and 1.630 eV (B), and a weaker, broad signal at about 1.59 eV (d). For comparison purposes, Fig. 4(b) shows the PL and PLE spectra recorded in bare GaAs NWs having a *pure ZB* phase. Unfortunately, the signal is rather weak in these ZB NWs and results in a noisy PLE spectrum. Nevertheless, the lowest-energy resonance in PLE is peaked at 1.516 eV, very close to that expected for bulk ZB GaAs (the Stokes shift is 1 meV, larger than in WZ-like samples), and no clear resonance is observed at higher energies. The spectrum in

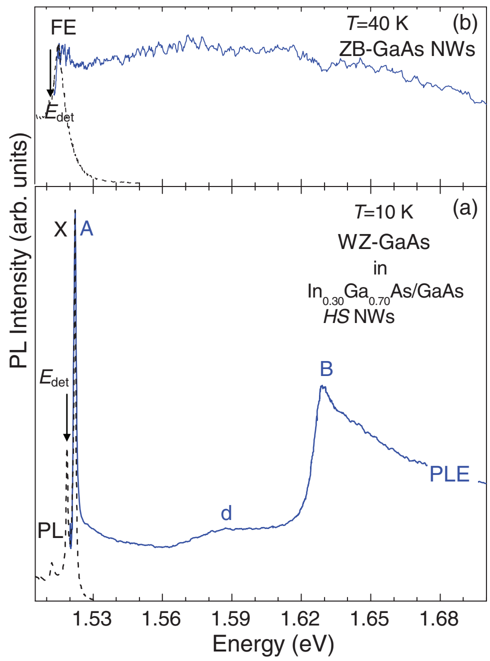

FIG. 4. (Color online) (a) PL (black dashed line) and PL excitation (blue solid line) spectra at $T = 10$ K of a WZ GaAs section in an $In_xGa_{1\text{-}x}As$/GaAs ($x = 0.30$) heterostructure NW sample. The measurements were recorded in a backscattering geometry. The arrow points to the PLE detection energy (Y_2 peak). (b) PLE spectrum at $T = 40$ K in ZB GaAs self-induced NWs. The arrow points to the PLE detection energy ($E_{det} = 1.511$ eV). Notice the absence of any resonance at an energy higher than that of the free exciton.

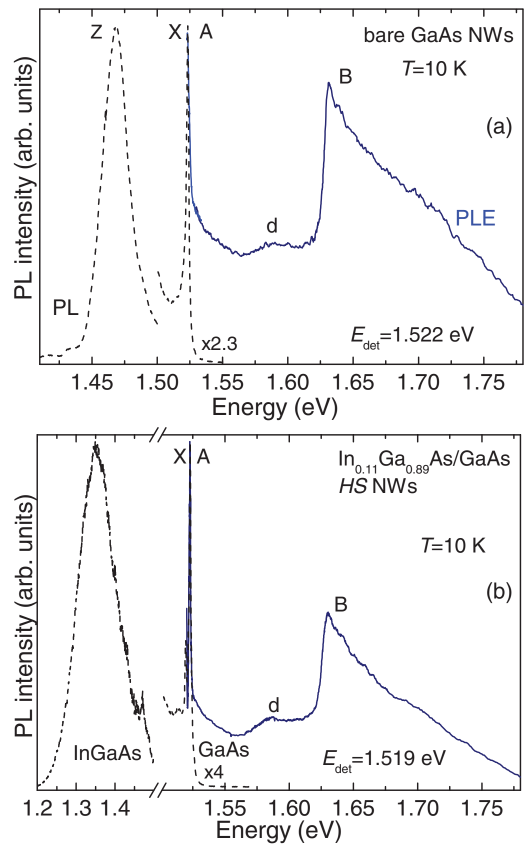

FIG. 5. (Color online) (a) PL (black dashed lines) and PL excitation (PLE, blue solid lines) spectra of bare GaAs NWs at $T = 10$ K. (b) The same for $In_xGa_{1\text{-}x}As$/GaAs heterostructure NWs ($x = 0.11$). The PLE detection energy is reported in the figure. The measurements were recorded in a backscattering geometry.

Fig. 4(b) is taken at 40 K in order to minimize contributions from defect-related states.

The main features of the PLE spectrum shown in Fig. 4(a) do not depend on the presence of the InGaAs section or on its composition. Indeed, Fig. 5 displays the PL and PLE spectra of bare GaAs NWs and of the GaAs section in $In_xGa_{1\text{-}x}As$/GaAs HS NWs with $x = 0.11$. We point out that the energy of the emission line X and absorption lines A, B, and d in the InGaAs/GaAs NWs are the same as those in the bare GaAs NWs, which are virtually strain free, and that very narrow X lines are observed in both cases. This rules out any major role played by strain in determining the energies of those transitions. The absence of such a contribution is likely due to sufficiently thick GaAs tips that permit to accommodate the strain. The extremely good optical properties of the samples are also supported by the negligibly small Stokes shift (∼0.1 meV) between the X peak in PL and the A peak in PLE observed for both InGaAs/GaAs and bare GaAs NWs. Considering all samples measured, we find $A = (1.5226\text{–}1.5241)$ eV, $B = (1.6293\text{–}1.6323)$ eV, and $B - A = (106.7\text{–}108.7)$ meV.

Other important information is deduced from the temperature dependence of the two bands A and B. Figure 6 shows the PL (black dashed lines) and PLE (red solid lines) spectra relative to the A (or X) and B transitions, respectively, at three temperatures recorded in a HS $In_{0.3}Ga_{0.7}As$-GaAs sample. Both transitions have a regular, Varshni-like energy shift with T (not shown here), which supports their intrinsic nature. The energy of the X band taken at room temperature (1.434 eV) is ∼10 meV greater than that of the corresponding band measured in ZB GaAs (not shown here). It is interesting to note that band B is observed in the PL spectrum at room temperature despite its large energy distance from the ground state (107 meV). This suggests a quite high carrier temperature, but this point deserves further detailed investigations.

Let us focus on the symmetry properties of the different resonances observed in Figs. 4 and 5. Figure 7 displays the dependence of the PLE spectra on the polarization of the exciting photons. In particular, the laser was steered at grazing incidence on the sample surface (namely, perpendicular to the NW axis) and the emitted light was collected in the direction perpendicular to the sample surface (namely, in the direction of the NW axis). The inset shows PLE spectra taken at 10 K in this geometry for either laser polarization parallel, $\varepsilon_\parallel$, or perpendicular, $\varepsilon_\perp$, to the NW axis. Resonances A and B are very well defined for both polarizations. Resonance A, together with its continuum, is stronger when the absorbed light is polarized perpendicularly to the NW axis, while resonance B and its continuum show a much weaker dependence on the exciting light polarization. Finally, the polarization dependence of the d band can be hardly disentangled from the strong background due to band A. The detailed dependence of the absorption signal on polarization is shown in the main part of Fig. 7, where the polarization degree of the emitted light intensity, $\rho = (I_\perp - I_\parallel)/(I_\perp + I_\parallel)$, is plotted as a function of

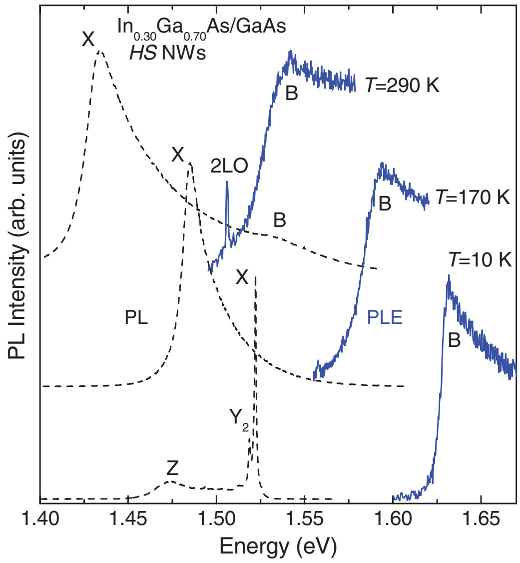

FIG. 6. (Color online) PL (black dashed lines) and PL excitation (PLE, blue solid lines) spectra of a WZ GaAs section in an $In_xGa_{1-x}As/GaAs$ ($x = 0.30$) heterostructure NW sample at three different temperatures. The detection energy was set at the X peak. The measurements were recorded in a backscattering geometry. At each temperature, the detection energy in the PLE spectrum has been that of the X-band peak in PL, where X indicates free-exciton and/or free-carrier recombination. The line labeled 2LO, at 2×36 meV from the PLE detection energy, is due to Raman scattering in GaAs involving two longitudinal optical phonons.

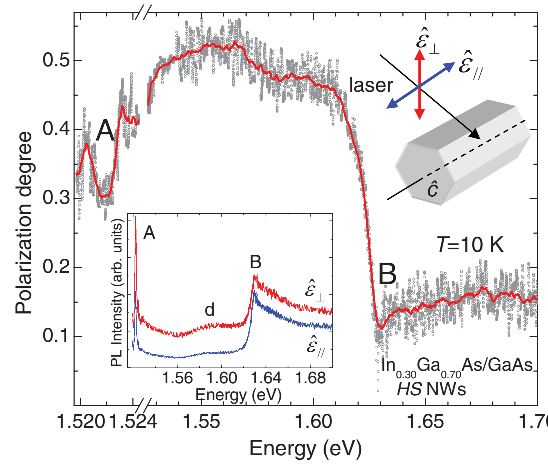

FIG. 7. (Color online) Degree of polarization $\rho = (I_\perp - I_\parallel)/(I_\perp + I_\parallel)$ of the PLE signal (gray line; the red line is a smoothing curve) at $T = 10$ K of a WZ GaAs section in an $In_xGa_{1-x}As/GaAs$ ($x = 0.30$) heterostructure NW sample. $I_\perp$ and $I_\parallel$, shown in the bottom left-hand inset, are the PLE intensities for polarization of the exciting photons perpendicular and parallel, respectively, to the wire $\hat{c}$ axis (see the sketch in the top right-hand inset). The laser was steered at grazing incidence on the sample surface (namely, perpendicular to the NW axis) and the emitted light was collected in the direction perpendicular to the sample surface (namely, in the direction of the NW axis). Notice the axis break and change of scale on the abscissa axis. The attributions of A, B, and d are discussed in the text.

the exciting photon energy. $I_\parallel$ and $I_\perp$ are the PL intensity for $\varepsilon_\parallel$ and $\varepsilon_\perp$, respectively. ρ is maximum ($\sim$0.5) up to the energy corresponding to the B peak and it reduces abruptly to less than one third ($\sim$0.15) for energies greater than 1.630 eV. This residual polarization is due to the signal arising from the polarized background of band A. A shallow minimum is observed in resonance with both A and B peaks, as if the exciton interaction mixed, possibly mediated by surface fields, the different symmetries of the valence bands.

IV. DISCUSSION

We now come to summarize and discuss our data. We have shown that the PL and PLE signals found at energies above that of the FE in ZB GaAs (1.515 eV) are due to *e-h* recombination involving WZ GaAs. Let us now assume that the X line in PL and the A line in PLE correspond to the Γ_{9v}-Γ_{7c} free-exciton recombination and absorption, respectively, as indicated by the polarization selection rules for band-band transitions in WZ structures. On the same ground, the B line in PLE corresponds to the Γ_{7vu}-Γ_{7c} free-exciton absorption. Indeed, transitions involving the Γ_{9v} valence band are permitted only for perpendicular polarization, while those involving the Γ_{7vu} are permitted for both parallel (by spin-orbit interaction) and perpendicular polarization (see Fig. 7).[21,22] The energy difference between the A and B transitions, 107 meV, agrees with that found by Ketterer *et al.*[18] for the Γ_{9v}-Γ_{7vu} energy difference, while it is larger than the value, 65 meV, found by Kusch *et al.*[17] for this same energy difference. Within the above picture, the weak d line could correspond to the Γ_{9v}-Γ_{8c} transition,[38] whose spin-orbit interaction permits only for perpendicular polarization.

Theoretical calculations[26,30] suggest a type-II alignment at WZ-ZB interfaces and broad bands, observed in WZ-ZB InP disordered superlattices,[39,40] have been attributed to type-II transitions because of a large blueshift for increasing excitation power. We remark that such a blueshift is not observed for the X line that is very stable for increasing excitation power and shows a usual Varshni shift in temperature. Therefore, the X line should be ascribed, most likely, to a type-I free exciton. Also, we point out that the energy of the X line remains the same on a *same* sample, while it varies by roughly ± 1 meV (average value 1.523 eV) from sample to sample. Therefore, extrinsic factors strictly related to the specific sample may influence the X-line energy. For instance, the 1.526 eV line observed above the X line (see Fig. 1) could originate from some NWs influenced by surface-related effects or by confinement (the very low intensity of this line and its absence in μ-PL and PLE spectra indicate, however, a negligibly small statistical occurrence of this transition).

Although most of the experimental features reported above suggest that 1.523 eV would be the excitonic band-gap value of WZ GaAs at $T = 10$ K, this assignment ought to be critically discussed in light of those theoretical and experimental results in the GaAs NW literature pointing toward band-gap energies higher than 1.523 eV.[14–20] On the theoretical side, the band-gap energy difference $\Delta E_{\mathrm{WZ\text{-}ZB}}$ we found ($\sim$10 meV as measured at room temperature, which permits to disregard excitonic effects) does not match well the theoretical estimate of

$\Delta E_{\text{WZ-ZB}} = 32$ meV, recently determined by state-of-the-art quasiparticle calculations beyond the density-functional theory and including a spin-orbit interaction.[26] This discrepancy could suggest an attribution of the X line to FE transitions in different GaAs phases with smaller band-gap energies, e.g., the $6H$ and $4H$. However, the value of $\sim$107 meV for the Γ_{9v}-Γ_{7vu} energy difference points toward a WZ $2H$ phase.[41] Moreover, high-resolution TEM results show that these phases are not sizably present in our NWs.

On the experimental side, recent PL,[14] cathodoluminescence,[15] and PV[20] measurements would support the PLE signal centered at about 1.59 eV (band d in Figs. 4, 5, and 7) as the band-gap energy of WZ GaAs, namely, 70 meV above the ZB band gap. However, even this attribution cannot be robust because of the broadness of that resonance as well as of its small intensity, namely, its small density of states.

On the grounds of the above arguments and of PL and cathodoluminescence spectra showing lines and bands, respectively, peaked at energies higher than that of the X and A lines, it is hard to make an unquestionable attribution of the observed recombination and absorption signals, although recorded in samples with high optical quality, as demonstrated by the extremely narrow FWHM of the X (A) line. Present and literature results seem to suggest that establishing the band-gap energy of *bulk* WZ GaAs by investigating the properties of WZ GaAs *nanowires* may be misleading: Several extrinsic or intrinsic effects (such as mixed phases, defects, surface electric fields, different ZB-WZ combinations, or the existence of $6H$ and $4H$ polytypes) can, to a different extent, influence the properties of NWs.

V. CONCLUSIONS

PL and PLE of GaAs NWs and InGaAs/GaAs heterostructure NWs have shown extremely narrow excitonic lines at energies above the ZB GaAs band gap. Those transitions can be easily followed up to room temperature. The polarization properties of these transitions allow us to associate them to free excitons involving wurtzite GaAs valence bands. At room temperature, we find that the PL emission X is $\sim$10 meV higher in energy than in ZB GaAs. However, a straightforward, robust attribution on the basis of the mere experimental results of that sharp transition to the excitonic fundamental band gap in pure wurtzite *bulklike* GaAs is made quite difficult by a comparison with the existing literature. Therein, indeed, slightly smaller or much higher values of the energy gap are reported in nanowire structures seemingly showing a pure WZ phase as well. Nevertheless, our work demonstrates that the optical quality of the samples and, in particular, the linewidth of the luminescence, can be of the highest quality despite the presence of lattice imperfections.

ACKNOWLEDGMENT

The authors acknowledge fruitful discussions with P. Alippi, V. Fiorentini, A. Zunger, L. Geelhar, F. Bechstedt, and W. R. L. Lambrecht.

*faustino.martelli@cnr.it

[1] K. Hiruma, M. Yazawa, K. Haraguchi, K. Ogawa, T. Katsuyama, M. Koguchi, and H. Kakibayashi, J. Appl. Phys. **74**, 3162 (1993).

[2] H. Shtrikman, R. Popovitz-Biro, A. Kretinin, L. Houben, M. Heiblum, M. Bukała, M. Galicka, R. Buczko, and P. Kacman, Nano Lett. **9**, 1506 (2009).

[3] A. D. Kimberly, C. Thelander, L. Samuelson, and P. Caroff, Nano Lett. **10**, 3494 (2010).

[4] E. G. Gadret, G. O. Dias, L. C. O. Dacal, M. M. de Lima, Jr., C. V. R. S. Ruffo, F. Iikawa, M. J. S. P. Brasil, T. Chiaramonte, M. A. Cotta, L. H. G. Tizei, D. Ugarte, and A. Cantarero, Phys. Rev. B **82**, 125327 (2010).

[5] A. Mishra, L. V. Titova, T. B. Hoang, H. E. Jackson, L. M. Smith, J. M. Yarrison-Rice, Y. Kim, H. J. Joyce, Q. Gao, H. H. Tan, and C. Jagadish, Appl. Phys. Lett. **91**, 263104 (2007).

[6] M. Mattila, T. Hakkarainen, M. Mulot, and H. Lipsanen, Nanotechnology **17**, 1580 (2006).

[7] M. Heiss, S. Conesa-Boj, J. Ren, H.-H. Tseng, A. Gali, A. Rudolph, E. Uccelli, F. Peirò, J. R. Morante, D. Schuh, E. Reiger, E. Kaxiras, J. Arbiol, and A. Fontcuberta i Morral, Phys. Rev. B **83**, 045303 (2011).

[8] M. Moewe, L. C. Chuang, S. Crankshaw, C. Chase, and C. Chang-Hasnain, Appl. Phys. Lett. **93**, 023116 (2008).

[9] L. C. Chuang, M. Moewe, K. W. Ng, T.-T. Tran, S. Crankshaw, R. Chen, W. S. Ko, and C. Chang-Hasnain, Appl. Phys. Lett. **98**, 123101 (2011).

[10] A. Lugstein, A. Maxwell Andrews, M. Steinmair, Y.-J. Hyun, E. Bertagnolli, M. Weil, P. Pongratz, M. Schramböck, T. Roch, and G. Strasser, Nanotechnology **18**, 355306 (2007).

[11] B. Ketterer, M. Heiss, M. M. Livrozet, E. Reiger, and A. Fontcuberta i Morral, Phys. Rev. B **83**, 125307 (2011).

[12] L. Ahtapodov, J. Todorovic, P. Olk, T. Mjåland, P. Slåttnes, D. L. Dheeraj, A. T. J. Helvoort, B.-O. Fimland, and H. Weman, Nano Lett. **12**, 6090 (2012).

[13] F. Martelli, M. Piccin, G. Bais, F. Jabeen, S. Ambrosini, S. Rubini, and A. Franciosi, Nanotechnology **18**, 125603 (2007).

[14] S.-G. Ihn, M.-Y. Ryub, and J.-I. Song, Solid State Commun. **150**, 729 (2010).

[15] U. Jahn, J. Lähnemann, C. Pfüller, O. Brandt, B. Jenichen, M. Ramsteiner, L. Geelhaar, and H. Riechert, Phys. Rev. B **85**, 045323 (2012).

[16] T. B. Hoang, A. F. Moses, H. L. Zhou, D. L. Dheeraj, B. O. Fimland, and H. Weman, Appl. Phys. Lett. **94**, 133105 (2009).

[17] P. Kusch, S. Breuer, M. Ramsteiner, L. Geelhar, H. Riechert, and S. Reich, Phys. Rev. B **86**, 075317 (2012).

[18] B. Ketterer, M. Heiss, E. Uccelli, J. Arbiol, and A. Fontcuberta i Morral, ACS Nano **5**, 7585 (2011).

[19] W. Peng, F. Jabeen, B. Jusserand, J. C. Harmand, and M. Bernard, Appl. Phys. Lett. **100**, 073102 (2012).

[20] R. Gurwitz, A. Tavor, L. Karpeles, I. Shalish, W. Yi, G. Seryogin, and V. Narayanamurti, Appl. Phys. Lett. **100**, 191602 (2012).

[21] J. L. Birman, Phys. Rev. **114**, 1490 (1959).

[22] P. Tronc, Yu. E. Kitaev, G. Wang, M. F. Limonov, A. G. Panfilov, and G. Neu, Phys. Status Solidi B **216**, 599 (1999).
[23] C.-H. Yeh, S.-H. Wei, and A. Zunger, Phys. Rev. B **50**, 2715 (1994).
[24] Z. Zanolli, F. Fuchs, J. Furtmüller, U. von Barth, and F. Bechsted, Phys. Rev. B **75**, 245121 (2007).
[25] P. Alippi and V. Fiorentini (private communication).
[26] A. Belabbes, C. Panse, J. Furthmüller, and F. Bechstedt, Phys. Rev. B **86**, 075208 (2012).
[27] T. Cheiwchanchamnangij and W. R. L. Lambrecht, Phys. Rev. B **84**, 035203 (2011).
[28] A. De and C. E. Pryor, Phys. Rev. B **81**, 155210 (2010).
[29] J.-M. Jancu, K. Gauthron, L. Largeau, G. Patriarche, J.-C. Harmand, and P. Voisin, Appl. Phys. Lett. **97**, 041910 (2010).
[30] M. Murayama and T. Nakayama, Phys. Rev. B **49**, 4710 (1994).
[31] F. Jabeen, S. Rubini, V. Grillo, L. Felisari, and F. Martelli, Appl. Phys. Lett. **93**, 083117 (2008).
[32] R. E. Nahory, M. A. Pollack, W. D. Johnson, Jr., and R. L. Barns, Appl. Phys. Lett. **33**, 659 (1978).
[33] D. Spirkoska, J. Arbiol, A. Gustafsson, S. Conesa-Boj, F. Glas, I. Zardo, M. Heigoldt, M. H. Gass, A. L. Bleloch, S. Estrade, M. Kaniber, J. Rossler, F. Peiro, J. R. Morante, G. Abstreiter, L. Samuelson, and A. Fontcuberta i Morral, Phys. Rev. B **80**, 245325 (2009).
[34] L. Fang, X. Zhao, Y.-H. Chiu, D. Ko, K. M. Reddy, T. R. Lemberger, N. P. Padture, F. Yang, and E. Johnston-Halperin, Appl. Phys. Lett. **99**, 141101 (2011).
[35] F. Jabeen, S. Rubini, V. Grillo, and F. Martelli, IEEE J. Sel. Top. Quantum Electron. **17**, 794 (2011).
[36] A. Convertino, M. Cuscunà, S. Rubini, and F. Martelli, J. Appl. Phys. **111**, 114302 (2012).
[37] M. De Luca, A. Polimeni, M. Felici, A. Miriametro, M. Capizzi, F. Mura, S. Rubini, and F. Martelli, Appl. Phys. Lett. **102**, 173102 (2013).
[38] M. Cardona and G. Harbeke, Phys. Rev. **137**, A1467 (1965), and references therein.
[39] J. Bao, D. C. Bell, F. Capasso, J. B. Wagner, T. Mårtensson, J. Trägårdh, and L. Samuelson, Nano Lett. **8**, 836 (2008).
[40] K. Pemasiri, M. Montazeri, R. Gass, L. M. Smith, H. E. Jackson, J. Yarrison-Rice, S. Paiman, Q. Gao, H. Hoe Tan, C. Jagadish, X. Zhang, and J. Zou, Nano Lett. **9**, 648 (2009).
[41] D. Spirkoska, Al. L. Efros, W. R. L. Lambrecht, T. Cheiwchanchamnangij, A. Fontcuberta i Morral, and G. Abstreiter, Phys. Rev. B **85**, 045309 (2012).